SUPPORTING INFORMATION

Solubilization of Pyridone-Based Fluorescent Tag by Complexation in Cucurbit[7]uril

Reem H. Alzard,[†] Muna S. Bufaroosha,[†] Noura Al-Shamsi,[†] Amir Sohail,[†] Naji Al-Dubaili,[†] Alaa A. Salem,[†] Ibrahim M. Abdou,[†] and Na'il Saleh*[†]

[†]*Chemistry Department, College of Science, United Arab Emirates University, P. O. Box 15551, Al-Ain, United Arab Emirates*

TABLE OF CONTENTS

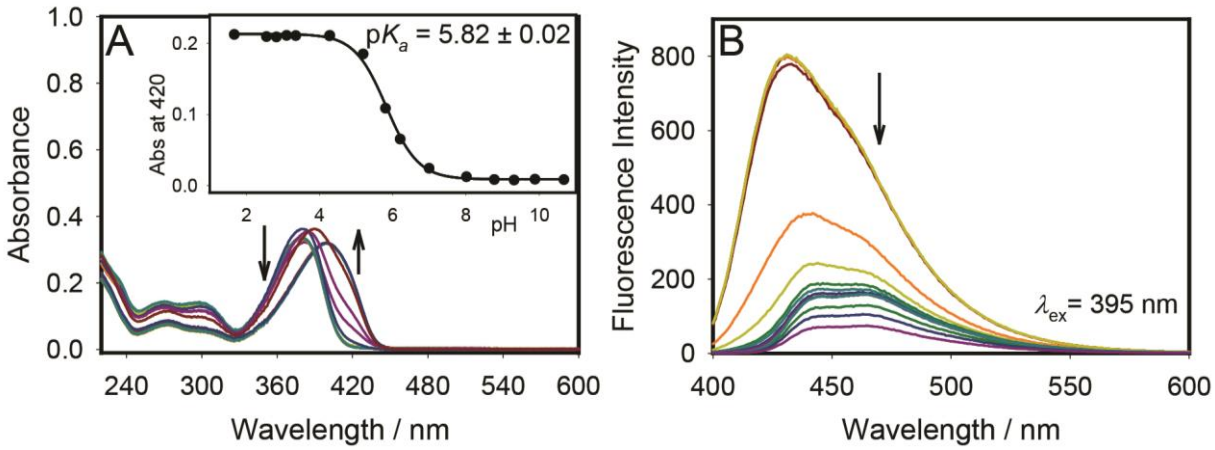

Figure S1. pH titration of TFP: panel A shows the evolution of the UV-Vis absorption spectra of TFP (40 μmol/L) as a function of HCl, together with the corresponding Henderson-Hasselbalch sigmoidal fit. Panel B shows the corresponding changes in emission spectra of TFP (40 μmol/L) as a function of pH, λ_{exc} = 395 nm.

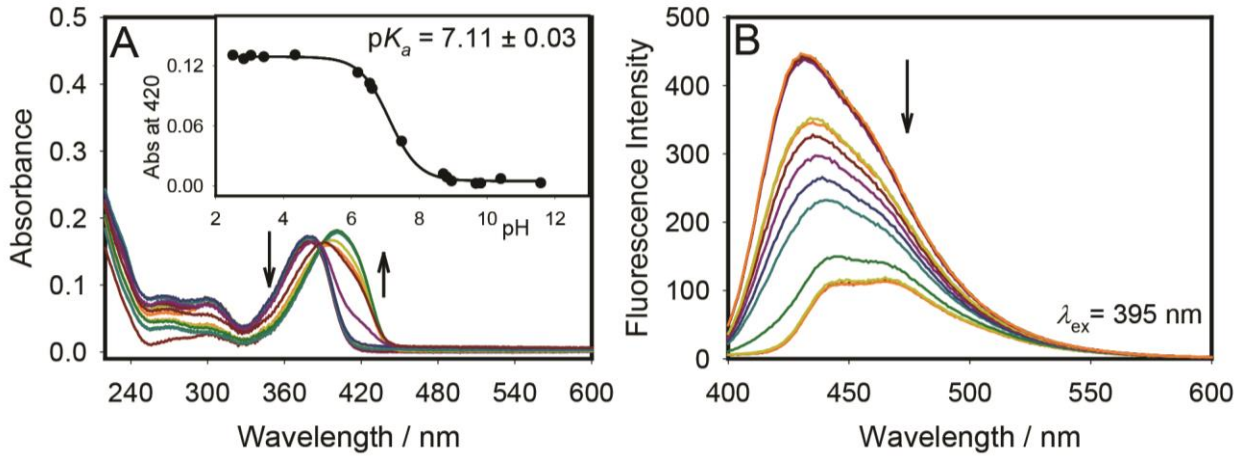

Figure S2. pH titration of TFP: panel A shows the evolution of the UV-Vis absorption spectra of TFP (22 μmol/L) in the presence of CB7 (1 mmol/L) as a function of HCl, together with the corresponding Henderson-Hasselbalch sigmoidal fit. Panel B shows the corresponding changes in emission spectra of TFP (40 μmol/L) as a function of pH, λ_{exc} = 395 nm.

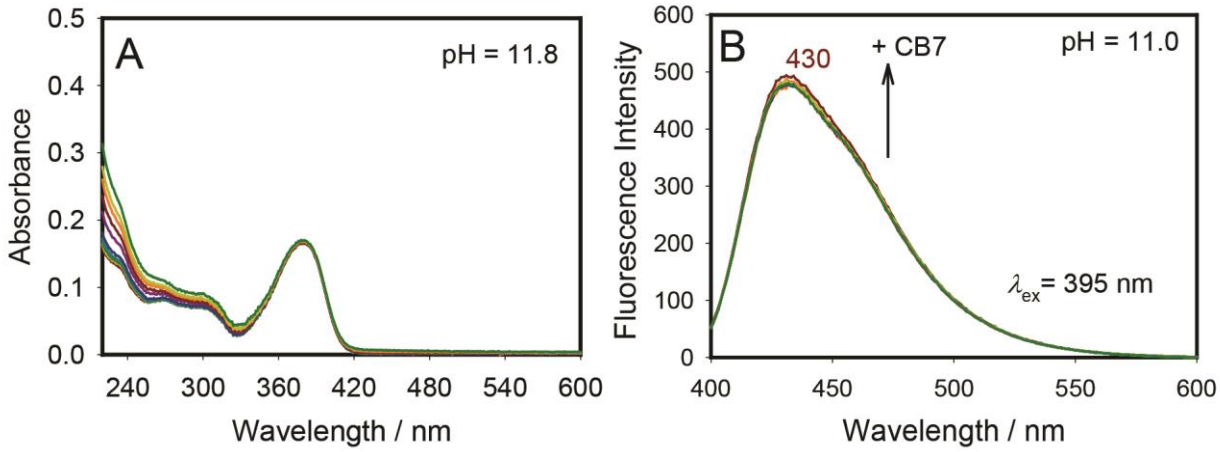

Figure S3. Binding titration of TFP with CB7 at pH 11: panel A shows no evolution of the UV-Vis absorption spectra of TFP (22 μmol/L) with the addition of CB7. Panel B shows the effects of binding to CB7 (0-300 μmol/L) on the emission spectra of TFP (22 μmol/L) at the same pH, λ_{exc} = 395 nm.

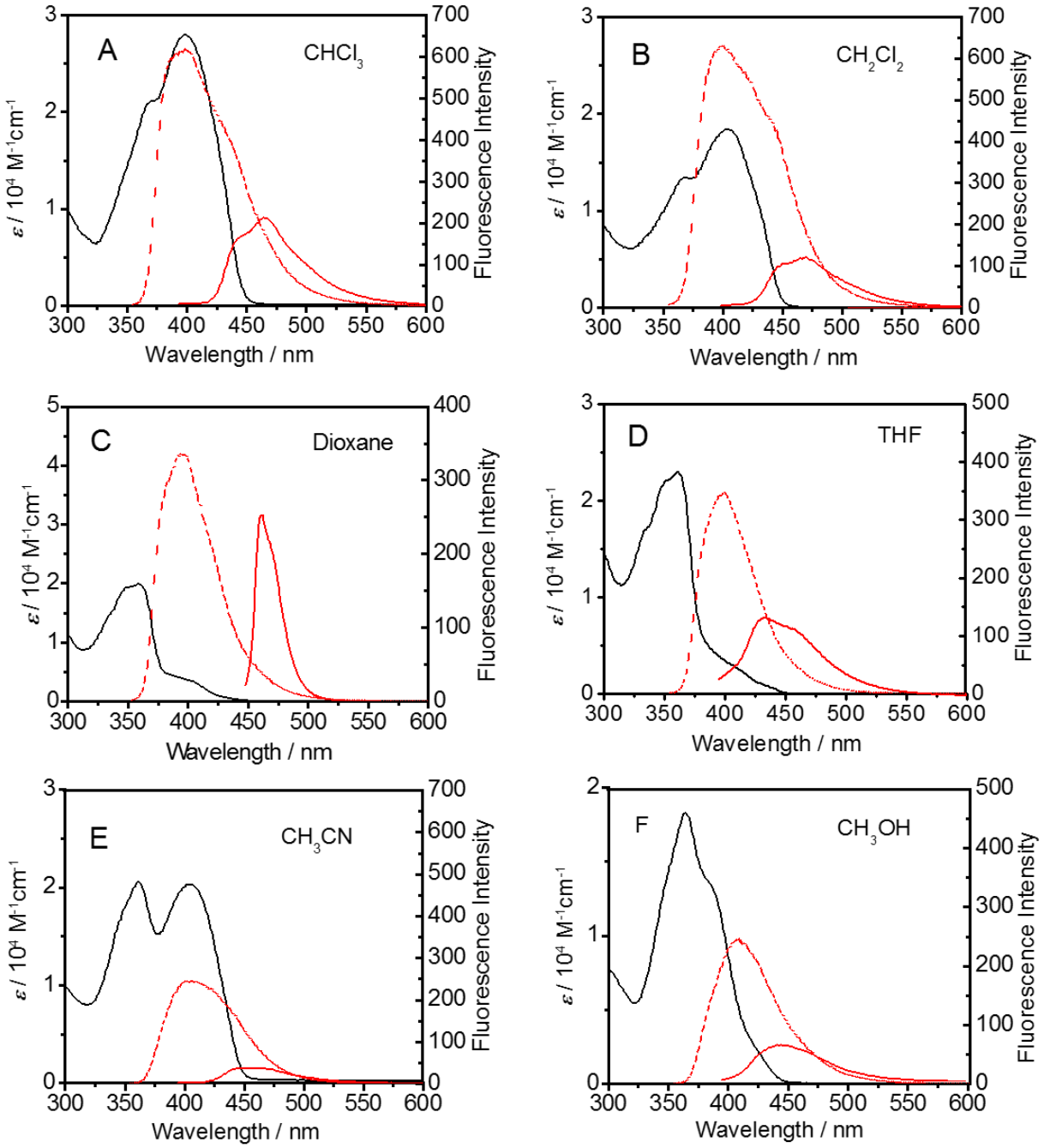

Figure S4. Absorption (black) emission (red) spectra (λ_{exc} = 350 nm for enol and 390 nm for keto) of TFP chromophores in different organic solvents in their keto (red solid line) and enol (red dashed line) forms; A: $CHCl_3$ = chloroform, B: CH_2Cl_2 = dichloromethane, C: $C_4H_8O_2$ = 1,4-dioxane, D: THF = tetrahydrofurane, E: CH_3CN = acetonitrile, and F: CH_3OH = methanol.

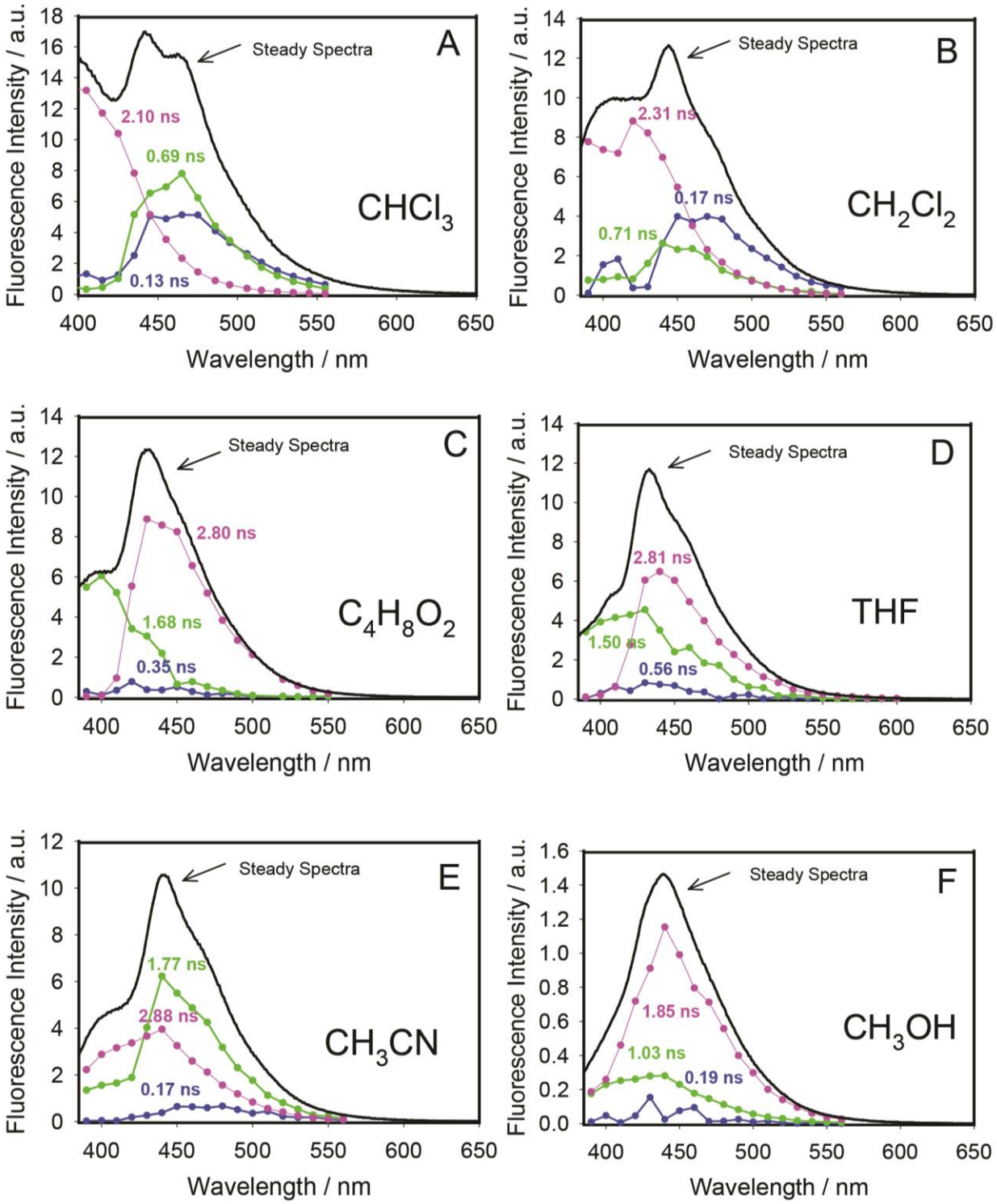

Figure S5. Decay-associated spectra (DAS) of three-component mixture of fluorophores for TFP (25 μM) in different organic solvents upon excitation at 375 nm and room temperature. The corresponding steady-state spectra of each solution are also shown for comparison (see experimental section); A: $CHCl_3$ = chloroform, B: CH_2Cl_2 = dichloromethane, C: $C_4H_8O_2$ = 1,4-dioxane, D: THF = tetrahydrofurane, E: CH_3CN = acetonitrile, F: CH_3OH = methanol, and G: CB7 = cucurbit[7]uril.

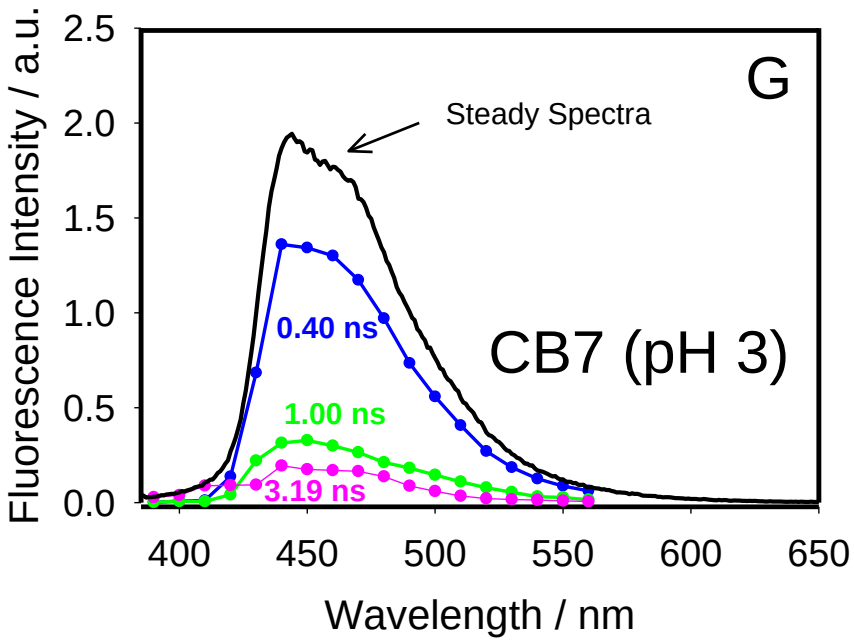

Figure S5. Continued.

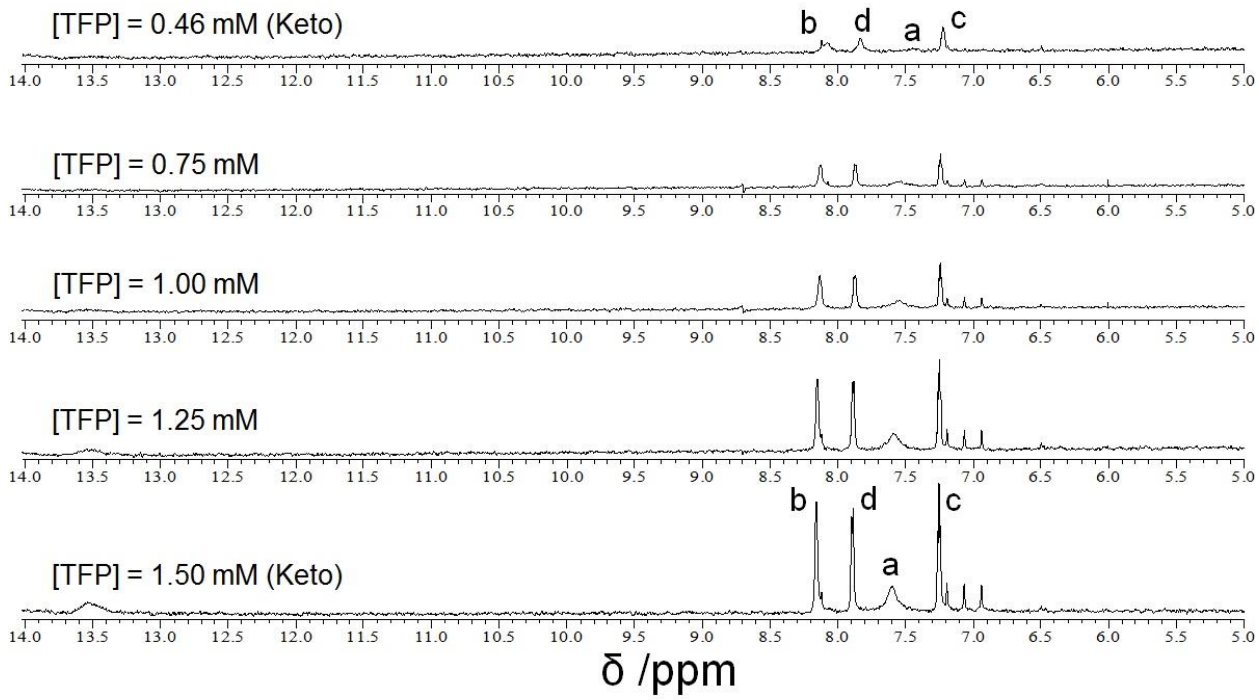

Figure S6. ^{1}H–NMR spectra of TFP in DMSO-d_6 at different concentrations. Assignments for peaks are indicated in experimental section.

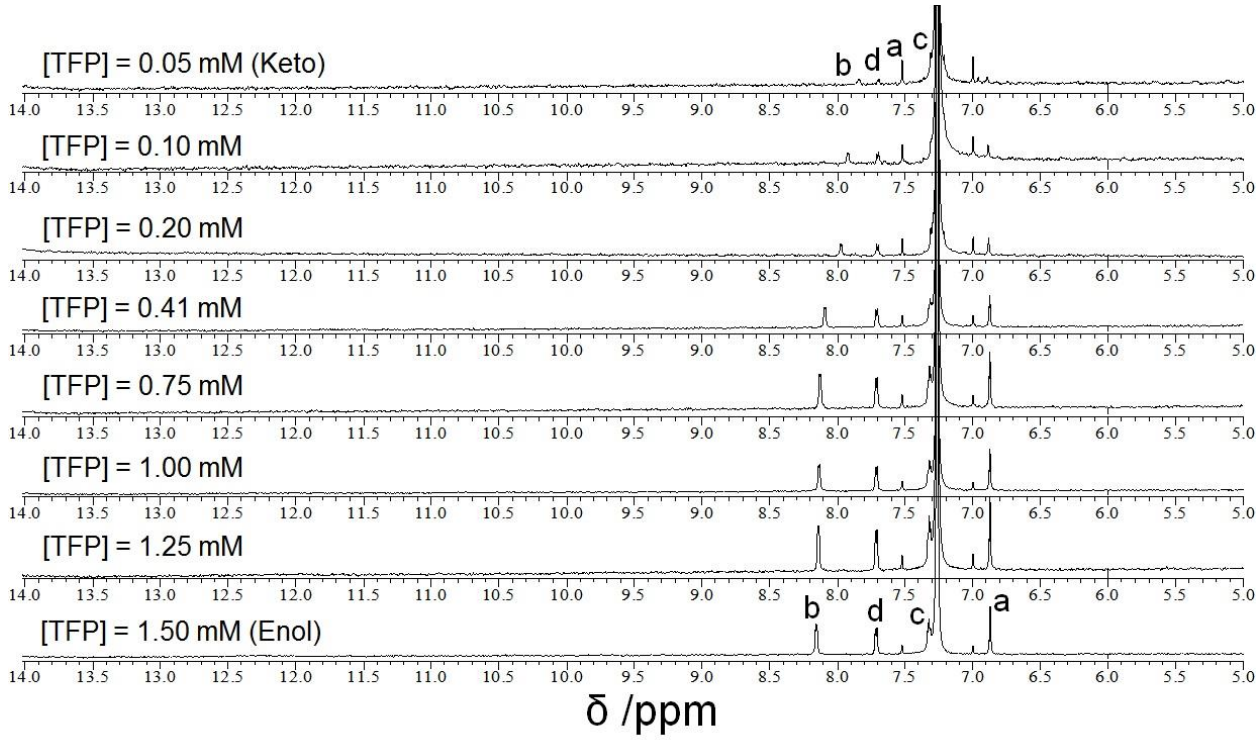

Figure S7. ^{1}H–NMR spectra of TFP in $CDCl_3$ at different concentrations. Assignments for peaks are indicated in experimental section.

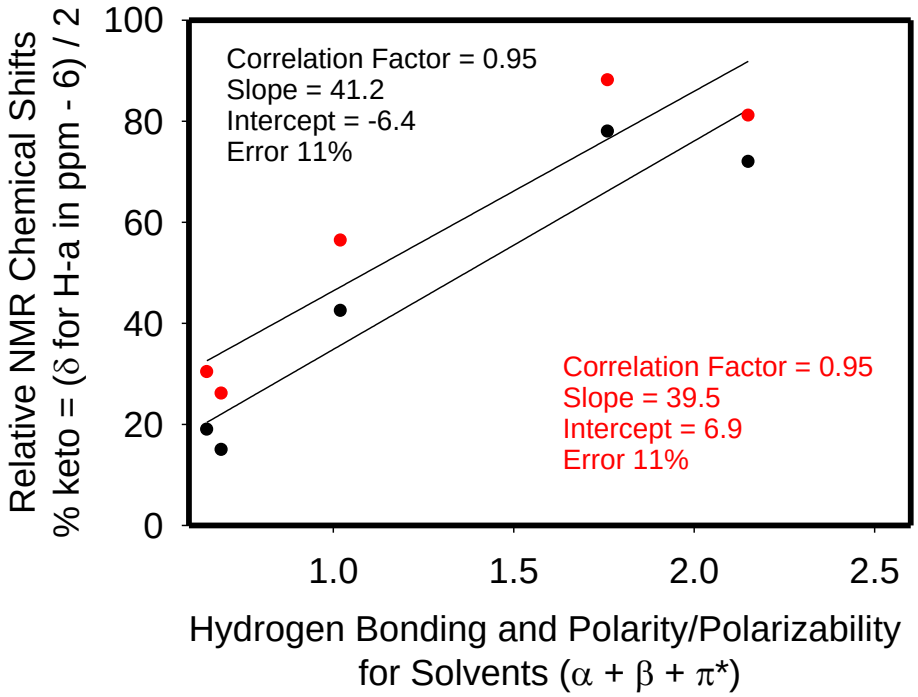

Figure S8. Correlation between the relative NMR chemical shifts for H-a proton in TFP with the sum of hydrogen bonding abilities and polarity/polarizability parameter ($\alpha + \beta + \pi^*$) for different solvents. The extrapolated plot for micromolar concentration is shown in red, see text.

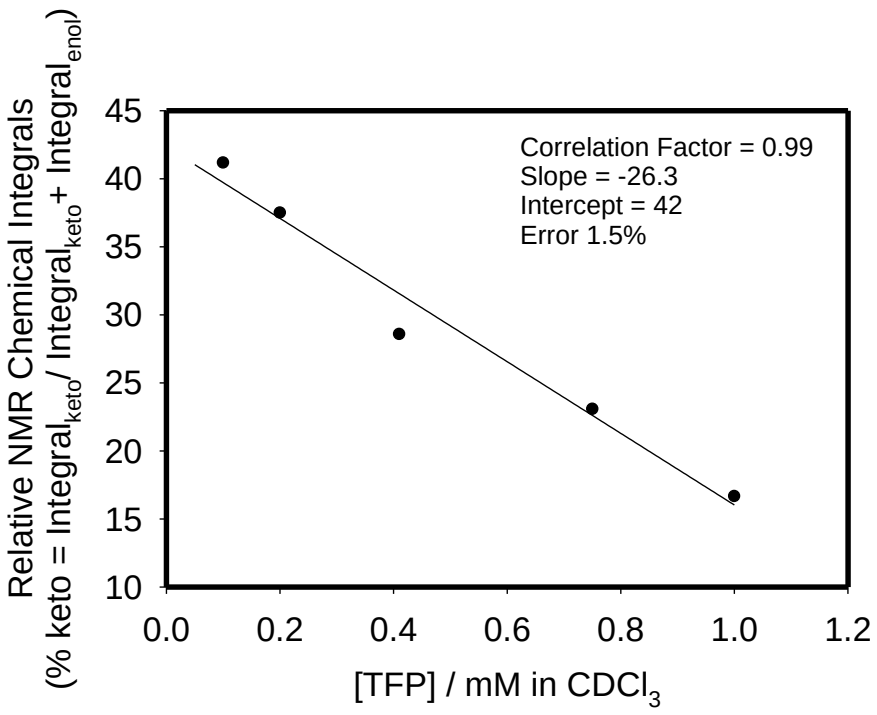

Figure S9. Correlation between the relative NMR chemical integrals for H-a proton in TFP (see Table S1) with the concentrations of TFP in millimolar in $CDCl_3$.

Table S1. The calculated percentage for keto form of TFP by using the integration areas for the NMR peaks of proton H_a at 6.9 ppm (enol) and 7.6 ppm (keto) and as a function of TFP concentrations in millimolar (mM).

TFP Concentration in $CDCl_3$ / mM	Integral area of enol signal	Integral area of keto signal	$\% \, keto = \frac{Integral\ area\ of\ keto\ signal}{Integral\ area\ of\ enol + Integral\ area\ of\ keto}$
0.05	1	1.5	60 (41 from extrapolation)
0.10	1	0.7	41
0.20	1	0.6	37
0.41	1	0.4	28
0.75	1	0.3	23
1.00	1	0.2	17
1.25	1	0.2	17
1.50	1	0.2	17